

# Vortex to Rotons Transition in Dipolar Bose-Einstein Condensates

Alberto Villois,<sup>1,2,3</sup> Miguel Onorato,<sup>3,4</sup> and Davide Proment<sup>1,2,5</sup>

<sup>1</sup>*School of Engineering, Mathematics and Physics, University of East Anglia,  
Norwich Research Park, Norwich, NR4 7TJ, United Kingdom*

<sup>2</sup>*Centre for Photonics and Quantum Science, University of East Anglia,  
Norwich Research Park, Norwich, NR4 7TJ, United Kingdom*

<sup>3</sup>*Dipartimento di Fisica, Università degli Studi di Torino, Via Pietro Giuria 1, 10125 Torino, Italy*

<sup>4</sup>*INFN, Sezione di Torino, Via Pietro Giuria 1, 10125 Torino, Italy*

<sup>5</sup>*ExtreMe Matter Institute EMMI, GSI Helmholtzzentrum fuer  
Schwerionenforschung, Planckstrasse 1, 64291 Darmstadt, Germany*

Recent experimental advancements enabled the creation of various systems exhibiting superfluid behavior, with one notable achievement being the development of dipolar Bose-Einstein condensates (dBECs). When confined along one or more spatial dimensions, these condensates exhibit a dispersion relation reminiscent of superfluid liquid helium, featuring a roton-like minimum. This study investigates the existence of two-dimensional solitary waves in dBECs characterised by topological defects (quantised vortices) and their transition to vortex-free Jones-Roberts solitons. The explicit connection between solitary waves and roton excitation is demonstrated, supporting Feynman's hypothesis regarding the nature of rotors as fading vortex excitations.

*Introduction.* Solitary waves stand out as a primary feature in nonlinear physics, finding application across diverse fields including fluid dynamics, optics, and plasma physics, while offering profound insights into the fundamental behaviour of complex systems. These self-sustaining wave patterns defy the typical dispersion expected in wave motion, maintaining their shape and velocity as they propagate through a medium. Their resilience against dispersion stems from a delicate balance between nonlinear and dispersive effects, making them stable entities within nonlinear systems.

Solitary waves characterized by the presence of vorticity hold particular significance within the field of quantum fluids, first discovered in the context of superfluid liquid helium [1]. Due to the topological nature of quantized vorticity, such structures play a fundamental role in the study of vortex dynamics and quantum turbulence [2]. Notable examples are the vortex ring cascade hypothesis in three dimensions superfluids [3, 4] and the Berezinskii-Kosterlitz-Thouless transition in two spatial dimensions [5]. Moreover, the study of such solitary waves have significantly contributed to the understanding of the nature of the superfluid. Specifically, the nucleation of solitary waves with quantized vorticity is believed, alongside nucleation of rotors, to be one of the possible mechanisms for breaking superfluidity in liquid helium, particularly in the low-pressure regime [6, 7].

The relationship between roton excitations and solitary waves has long been a subject of fascination. Particularly, Feynman postulated the origin of drag in a superfluid as the generation of roton excitations from a vanishing vortex ring [3], sparking numerous studies aimed at determining whether the energy and momentum of vortex rings were comparable to roton excitations. However, this hypothesis was disproved in the seminal work of Jones & Roberts [8]: With a weakly interacting model aimed to capture the key features of superfluid liquid helium, they conducted an investigation into the existence

of a family of axisymmetric solitary waves. These waves exhibit quantized vorticity at low speeds, taking the form of vortex rings in three dimensions and vortex dipoles in two dimensions. As their speed increases, they transition into vortex-free density dips, reaching speeds comparable to speed of phonons, the fastest excitations in the system before superfluidity breaks down [9].

Over the years, numerous experimental advancements have facilitated the generation of various systems exhibiting superfluid behavior, ranging from single and multi-component Bose-Einstein condensates (BECs) to spinor and Fermi gases. One of the most notable achievements was the development of BECs characterized by long-range dipole-dipole interactions, known as dipolar BECs (dBECs) [10, 11]. When one or more spatial dimensions are strongly confined, these condensates have elementary excitations which display a dispersion relation that, akin to superfluid liquid helium [12], features a roton minimum [13–15]. Such elementary excitations have been recently experimentally measured in dBECs [16, 17] and enabled the generation of a new supersolid state of matter [18–20]. Unlike liquid helium, cold gases allow for the direct visualization of small-scale vortex structures, as demonstrated recently [21–23]. Moreover, they can be accurately described by mean-field models based on the Gross-Pitaevskii equation. These properties make such systems particularly compelling for exploring the interplay between vortical structures and rotors.

In this Letter, we investigate the existence of two-dimensional solitary waves characterized by topological defects and their transition to vortex-free Jones-Roberts (JR) solitons in dBECs. The explicit connection between solitary waves and roton excitations is demonstrated for the first time, providing support for Feynman's hypothesis regarding the nature of rotors as fading vortex excitations.

*Theoretical model.* In the limit where the condensate is strongly confined along the  $z$ -direction with a character-

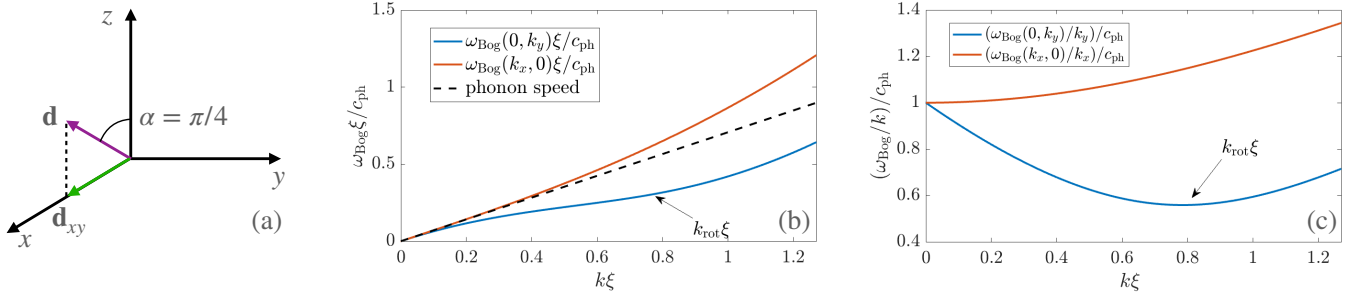


FIG. 1. In all plots we take  $\alpha = \pi/4$  and  $\beta = 0.9$ . (a) Sketch of the orientation of the dipole moment. (b) Bogoliubov dispersion relation along the  $k_x$  (red) and  $k_y$ -axis (blue). The phonon limit is shown with a dashed line. (c) Phase speed of the Bogoliubov excitations along the  $k_x$  (red) and  $k_y$ -axis (blue). The minimum value of each curve indicate the maximum speed allowed before breaking superfluidity.

istic confining length scale  $l_z$ , an excellent (quasi)-two-dimensional model with no confinement in the  $x$ - $y$  plane is given by the following Gross-Pitaevskii equation

$$i\hbar \frac{\partial \psi}{\partial t} = -\frac{\hbar^2}{2m} \nabla^2 \psi + g_c |\psi|^2 \psi + g_d \Phi \psi. \quad (1)$$

Here,  $\psi(x, y, t)$  is the two-dimensional order parameter,  $\nabla^2 = \partial_{xx} + \partial_{yy}$ ,  $g_c = 2\sqrt{2}\pi\hbar^2 a_s / (ml_z)$  is the contact (local) interaction coefficient,  $m$  and  $a_s$  are the mass and the s-wave scattering length of the boson, respectively, and  $g_d = |\mathbf{d}|^2 / \sqrt{2}\pi l_z$  is the dipole-dipole (nonlocal) interaction coefficient where  $\mathbf{d}$  is the dipole moment. The nonlocal dipolar interaction operator is defined as

$$\Phi = \frac{4\pi}{3} \mathcal{F}_{xy}^{-1} [\mathcal{F}_{xy} (|\psi|^2) F(\mathbf{q})] \quad (2)$$

where  $\mathcal{F}_{xy}(\cdot)$  is the spatial two-dimensional direct Fourier transform operator [24] and  $\mathbf{q} = \mathbf{k}l_z / \sqrt{2}$  is the wave vector on the  $x$ - $y$  plane. Without any loss of generality, we consider the dipole moment aligned with the  $x$ -axis and define  $\alpha$  being the angle between  $\mathbf{d}$  and the  $z$ -axis, see Fig. 1 (a). With this choice the function  $F(\cdot)$ , that represents the Fourier transform of the two-dimensional dipole-dipole interaction [15, 25], results in

$$F(\mathbf{q}) = \cos^2 \alpha F_{\perp}(q) + \sin^2 \alpha F_{\parallel}(q, q_x), \quad (3)$$

where  $q = |\mathbf{q}|$ ,  $q_x$  being the  $x$ -component of  $\mathbf{q}$ , and

$$F_{\perp}(q) = 2 - 3\sqrt{\pi} q e^{q^2} \operatorname{erfc}(q)$$

$$F_{\parallel}(q, q_x) = -1 + 3\sqrt{\pi} \frac{q_x^2}{q} e^{q^2} \operatorname{erfc}(q).$$

By assuming the homogeneous solution in the form

$$\psi(t) = \sqrt{n} e^{-i \frac{\mu t}{\hbar}} \quad (4)$$

where  $n$  is the average particle number density per unit of volume, one finds the chemical potential

$$\mu = g_c n \left[ 1 + (3 \cos^2 \alpha - 1) \frac{4\pi}{3} \beta \right], \quad \text{with } \beta = \frac{g_d}{g_c} \quad [26], \quad (5)$$

and its infinitesimal wave-like perturbations of wave-length  $\mathbf{k} = (k_x, k_y)$ , and angular frequency  $\omega_{\text{Bog}}$  to satisfy the Bogoliubov dispersion relation [15]

$$\omega_{\text{Bog}}(\mathbf{k}) = \pm \frac{|\mathbf{k}|}{\sqrt{m}} \sqrt{\frac{\hbar^2 |\mathbf{k}|^2}{4m} + g_c n \left[ 1 + \beta \frac{4\pi}{3} F\left(\frac{l_z \mathbf{k}}{\sqrt{2}}\right) \right]}. \quad (6)$$

Finally, by introducing the healing length,  $\xi = \hbar / \sqrt{2m\mu}$ , one finds the phonon speed (long wave perturbation) as  $c_{\text{ph}} = \sqrt{\mu/m}$ . One notices that, when  $\alpha \neq 0$ , Eq. (3) is anisotropic in  $\mathbf{k}$ , hence the Bogoliubov dispersion. Figure 1 (b) illustrates the two dispersion relation branches along the  $k_x$  and  $k_y$  directions, choosing  $\alpha = \pi/4$  and  $\beta = 0.9$ . For such values, used for all the results presented in this Letter, the dispersion relation along the  $k_x$  direction shows a point where the quantity  $\omega(k_x, 0)/k_x$  possesses a global minimum and corresponds to an analogue of the roton minimum measured in superfluid liquid helium, therefore called here *roton-like* minimum. Note that this minimum is present for a large range of  $(\alpha, \beta)$ , and our choice is achievable in experimental setups [10].

Taking advantage of the anisotropy of the dispersion relation, in this Letter we investigate the existence of solitary wave solutions in two-dimensional dBECs, their dependence on the alignment between their propagation velocity and the dipole moment, and revisit Feynman's hypothesis, originally formulated in superfluid liquid helium, on the vortex-roton transition. Jones & Roberts have demonstrated the existence of axisymmetric solitary waves within the Gross-Pitaevskii equation characterised only by contact interactions [8]. Their results were reproduced experimentally in [21]. In two dimensions, these solutions exhibit counter-rotating quantised vortices at low speeds that transition to density pulses free of topological defects at speeds comparable to the phonon speed. It is pedagogical to identify first the range of possible speeds at which a solitary travelling wave can propagate. To do so, one relies on the so-called band gap analysis introduced in [27]. The idea behind the band gap analysis is the following: a localised solitary wave (fully nonlin-

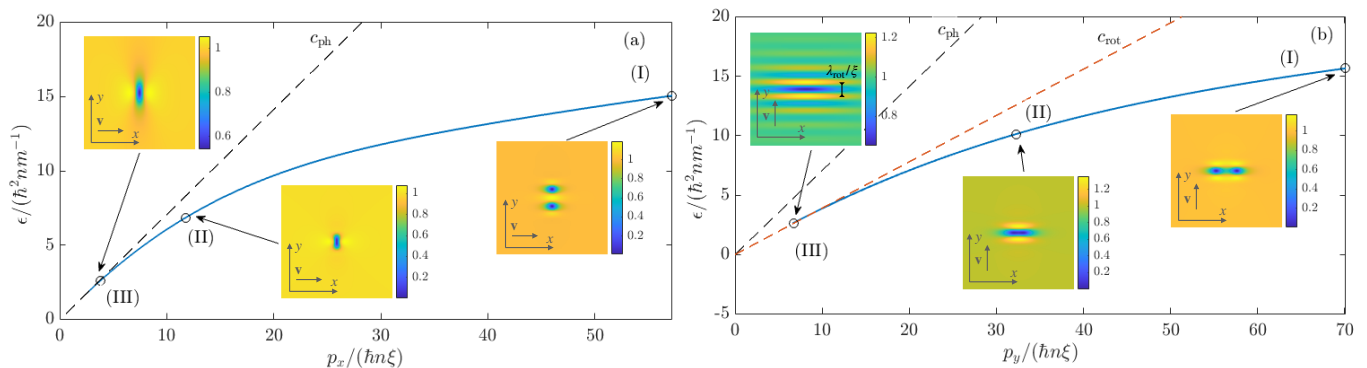


FIG. 2. The blue line shows the energy-momentum plot of solitary wave family moving along the  $x$  and  $y$ -directions, given in plots (a) and (b), respectively. Each point on the curve is a particular solitary wave whose speed is given by the slope of the tangent to the curve and its density profile  $|\psi|^2$ , rescaled by the average density  $n$  and zoomed around the localised density dip(s), is shown in the respective inset. The points (II) indicate where the transition between a vortex dipole to a JR soliton takes place. The black and red dashed lines represent the phonon and roton speed, respectively.

ear) excitation moving at velocity  $\mathbf{v} = (v_x, v_y)$  can exist on the top of the homogeneous solution (4) only if

$$\mathbf{v} \cdot \mathbf{k} \neq \omega_{\text{Bog}}(\mathbf{k}) \quad (7)$$

This is to prevent the resonant transfer of energy from the solitary wave to a Bogoliubov excitation. By using this criterion, it is straightforward to identify the range of speed values that the solitary wave is allowed, as shown in Fig. 1 (c). Note that Eq. (7) is equivalent to Landau's criterion for the breakdown of superfluidity, demonstrating that the along the  $x$ -direction superfluid excitations cannot move faster than the phonon speed, while along the  $y$ -direction the limiting speed is given by the roton speed  $c_{\text{rot}} = \min(\omega_{\text{Bog}}(0, k_y)/k_y)$  [28].

*Numerical methods.* The solitary wave solution is computed numerically by recasting the Gross-Pitaevskii equation (1) in the reference frame moving with velocity  $\mathbf{v}$  and seeking for a time-independent solution having the same chemical potential (5) of the homogeneous solution (4), see the SM for more details. The system is spatially discretized on a regular lattice with  $512^2$  collocation points over a box with size  $L_x/\xi = L_y/\xi = 80\pi$ . Periodic boundary conditions are considered in order to compute differential operators making use of Fourier spectral decomposition. The time-independent solution is found via a Newton-Raphson method, and the JR branch is followed by slowly varying the solitary wave speed. We also perform time evolutions of the time-dependent Gross-Pitaevskii equation (1) to analyse qualitatively the stability of the solitary wave; the time operator is resolved using a standard RK4 method. A thorough linear stability analysis is performed by looking at the spectral eigenvalues of the Bogoliubov-de Gennes (linearised) perturbations.

*Numerical results.* First, we investigate the family of solitary waves propagating along the direction of the dipole polarisation ( $x$ -direction), that is choosing  $v_y = 0$ . Each point on the blue line in Fig. 2 (a) represents the

energy-momentum coordinates of a solitary wave solution. The  $x$ -component of the velocity of each solitary wave is determined by the slope of this curve, as given analytically by  $v_x = \partial\epsilon/\partial p_x|_{v_y=0}$ , with  $\epsilon$  and  $p_x$  being the energy and  $x$ -component of the linear momentum densities of the solitary wave, respectively (see the SM for the mathematical derivation). Density profiles zoomed about the localised solitary wave are shown in the insets. Point (I) illustrates a vortex dipole (two topological defects in the argument of the order parameter, the order parameter goes to zero at the defect points), the transition between a solution with and without vorticity (no more topological defects, the order parameter still goes to zero) is indicated by point (II), point (III) shows a non-zero density dip in the order parameter. The vortex core density profiles in the dipole solution are elongated along the polarisation direction, in agreement with previous results [29, 30]. Here we show that such elongation is still present in the absence of vorticity, although it is lost in the limit for speeds approaching the phonon speed, see dashed black line in Fig. 2 (a), with a JR soliton resembling the typical profile of lump soliton solutions for the so-called Kadomtsev-Petviashvili equation [31].

We then explore the family of solitary waves moving perpendicularly to the direction of the dipole polarisation ( $y$ -direction), that is choosing  $v_x = 0$ , whose results are plotted in Fig. 2 (b). Here, the  $y$ -component of the velocity of each solitary wave is determined by the slope of this curve, resulting in  $v_y = \partial\epsilon/\partial p_y|_{v_x=0}$  where  $p_y$  is the  $y$ -component of the linear momentum density of the solitary wave. Again, density profiles zoomed about the localised waves are shown in the insets. Similarly to the previous case, both vortex dipole solutions and JR solitons have density profiles elongated along the polarisation direction, see point (I) and point (II) in Fig. 2 (b), respectively. However, in this case the JR solitons cannot approach the phonon speed resembling lump soliton solutions, as Landau's criterion for superfluidity breaking along the  $y$ -direction is now determined by the roton

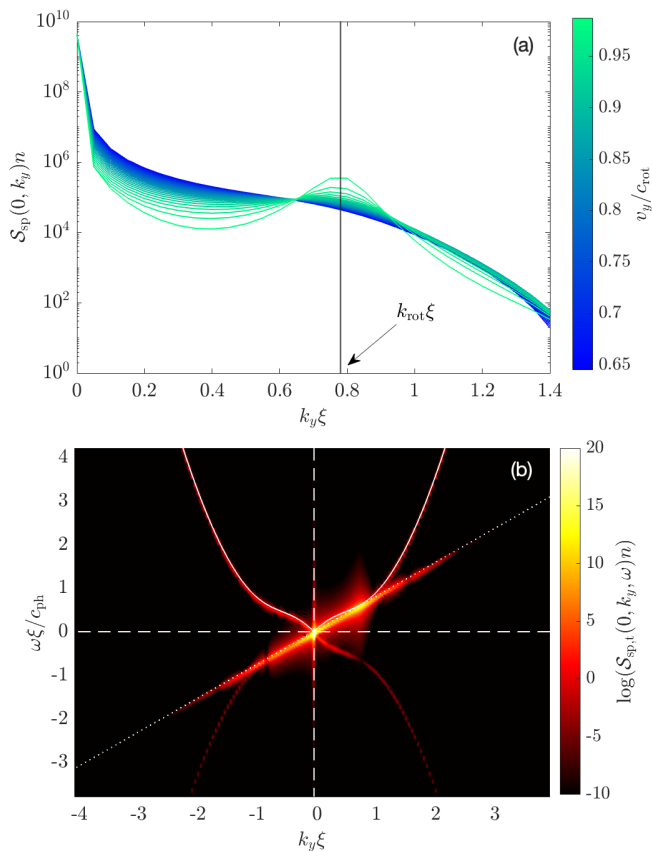


FIG. 3. (a) Spatial spectra  $\mathcal{S}_{\text{sp}}(k_x = 0, k_y)$  of the solitary wave solutions moving along the  $y$ -direction plotted for different  $v_y$  tending to the roton speed. (b) Spatio-temporal spectrum  $\mathcal{S}_{\text{sp},t}(k_x = 0, k_y, \omega)$  of the solitary wave solution associated to point (III) in Fig. 2 (b) with added white noise. The dynamics of such initial condition covers a distance roughly equal to the system size  $L_y$  and has being forced to be periodic in the long time interval  $\Delta$  by applying a standard double  $\tanh^2$  filter in order to make use of the Fast Fourier Transform when computing the time integral in the spatio-temporal spectrum.

speed, shown by a dashed red line in Fig. 2 (b). While approaching the roton speed, a transition from localised JR solitons to delocalised roton excitations appearing as stripes of characteristic scale  $\lambda_{\text{rot}} = 2\pi/k_{\text{rot}}$  becomes qualitatively visible, see point (III) in Fig. 2 (b).

To further characterise such a transition, we analyse the spectral properties of the solitary wave branch presented in Fig. 2 (b). Figure 3 (a) shows the collection of spatial spectra  $\mathcal{S}_{\text{sp}}(k_x, k_y) = |\mathcal{F}_{xy}(\psi_{\text{SW}})|^2$  plotted along the  $k_y$ -axis of the solitary waves found in Fig. 2 (b) for speeds,  $v_y/c_{\text{rot}} \geq 0.65$ . It is evident that a peak around the roton-like minimum wave number  $k_{\text{rot}}$  emerges and grows for growing speeds; this is a first indication that the travelling wave solution approaches the roton-like Bogoliubov excitation when its speed tends to the roton speed. To corroborate this claim we perform a time evolution of the fastest solitary wave solution, see point

(III) in Fig. 2 (b). White noise is added in the initial condition (noise to uniform solution ratio is order of  $10^{-4}$ ) to test the robustness of the localised wave,  $\psi_{\text{SW}+\text{N}} = \psi_{\text{SW}} + \text{noise}$ . After the solitary wave has evolved up to time  $t = \Delta$ , covering approximately a distance equal to the system size  $L_y$ , a spatio-temporal spectrum,  $\mathcal{S}_{\text{sp},t}(k_x, k_y, \omega) = |\int_0^\Delta \mathcal{F}_{xy}(\psi_{\text{SW}+\text{N}}) e^{i\omega t} dt|^2 / \Delta^2$ , is measured. Figure 3 (b) shows the spectral content of the signal onto the  $(k_y, \omega)$  plane identified by  $k_x = 0$ . The spectral content associated with the solitary wave corresponds to a straight signal, having slope equal to the solitary wave speed  $v_y$ , see dotted white line. Elementary excitations introduced by the presence of the noise in the initial condition, evolve according to the Bogoliubov dispersion, see solid white line. The Bogoliubov excitation branch almost meets the solitary wave signal at the roton-like wave number  $k_{\text{rot}}$ , indicating that a resonance will occur in the limit of the solitary wave speed tending to the roton speed. An animation in the SM shows the evolution of the density and phase fields covering a distance around  $20L_y$ , demonstrating visually that the solitary wave is preserved by the time evolution in presence of the added noise. A full Bogoliubov-de Gennes stability analysis, shown in the SM, has been carried out confirming the robustness of the solitary wave solutions with respect to noise.

*Conclusions and outlook.* In this Letter we demonstrated the existence of the Robert-Jones travelling wave solutions in two-dimensional dipolar condensates, showing that the solution branch is formed by a vortex dipole that continuously transits into a topologically-free density dip when exceeding a critical speed. The JR branch strongly depends on the alignment between the solitary wave velocity and the polarisation direction. When they are fully aligned, the JR soliton maximum speed tends to the phonon speed, like in standard (non-dipolar) condensates, while when they are completely orthogonal the limiting speed is the one given by the roton-like excitation. Note that in both cases the solitary wave excitation is subsonic and does not break the superfluidity as its velocity cannot be larger than the Landau's critical speed, which depends on the polarisation direction in dipolar condensates. Finally, we have investigated the fate of the JR soliton moving perpendicularly to the polarisation direction: at its speed increases the solution builds a spectral peak that tends to the roton-like Bogoliubov excitation, validating the analogy of Feynman's hypothesis regarding the nature of rotons as fading vortex excitations. Preliminary investigations on the stability of such JR solitons, both dynamically adding small-amplitude noise and semi-analytically within the linearised Bogoliubov-de Gennes framework, have shown that these solitary waves are robust and should be within the parameter range of feasibility in state-of-the-art dipolar gas experiments [32]. Open questions like how to generate such excitations, for example by moving an external potential, their scattering interaction, and the characterisation of their Landau's critical speed limit in terms

of Kadomtsev-Petviashvili-like solitons [31] will be the scope of the next publications.

### ACKNOWLEDGMENTS

M.O. was funded by Progetti di Ricerca di Interesse Nazionale (Grants No. 2020X4T57A and No. 2022WKRYNL) and by the Simons Foundation (Grant

No. 652354) D.P. would like to thank the Isaac Newton Institute for Mathematical Sciences for support and hospitality during the programme Dispersive hydrodynamics: mathematics, simulation and experiments when the final part of the work on this paper was undertaken. This work was supported by EPSRC Grant Number EP/R014604/1. This research was supported in part by the ExtreMe Matter Institute EMMI at the GSI Helmholtzzentrum fuer Schwerionenphysik, Darmstadt, Germany.

- 
- [1] R. J. Donnelly, *Quantized vortices in helium II*, Vol. 2 (Cambridge University Press, 1991).
- [2] P. M. Walmsley and A. I. Golov, *Phys. Rev. Lett.* **100**, 245301 (2008).
- [3] R. Feynman (Elsevier, 1955) pp. 17–53.
- [4] S. K. Nemirovskii, *Low Temperature Physics* **40**, 1116 (2014), <http://dx.doi.org/10.1063/1.4902230>.
- [5] Z. Hadzibabic and J. Dalibard, *La Rivista del Nuovo Cimento* **34**, 389 (2011).
- [6] G. G. Nancolas, T. Ellis, P. V. E. McClintock, and R. M. Bowley, *Nature* **316**, 797 (1985).
- [7] T. Ellis, P. V. E. McClintock, and W. F. Vinen, *Philosophical Transactions of the Royal Society of London. Series A, Mathematical and Physical Sciences* **315**, 259 (1985).
- [8] C. A. Jones and P. H. Roberts, *Journal of Physics A: Mathematical and General* **15**, 2599 (1982).
- [9] L. Pitaevskii and S. Stringari, *Bose-Einstein condensation and superfluidity*, Vol. 164 (Oxford University Press, 2016).
- [10] L. Chomaz, I. Ferrier-Barbut, F. Ferlaino, B. Laburthe-Tolra, B. L. Lev, and T. Pfau, *Reports on Progress in Physics* **86**, 026401 (2022).
- [11] N. Bigagli, W. Yuan, S. Zhang, B. Bulatovic, T. Karman, I. Stevenson, and S. Will, *Nature* **631**, 289 (2024).
- [12] H. Godfrin, K. Beauvois, A. Sultan, E. Krotscheck, J. Dawidowski, B. Fåk, and J. Ollivier, *Phys. Rev. B* **103**, 104516 (2021).
- [13] L. Santos, G. V. Shlyapnikov, and M. Lewenstein, *Phys. Rev. Lett.* **90**, 250403 (2003).
- [14] D. H. J. O’Dell, S. Giovanazzi, and G. Kurizki, *Phys. Rev. Lett.* **90**, 110402 (2003).
- [15] C. Ticknor, R. M. Wilson, and J. L. Bohn, *Phys. Rev. Lett.* **106**, 065301 (2011).
- [16] L. Chomaz, R. M. W. van Bijnen, D. Petter, G. Faraoni, S. Baier, J. H. Becher, M. J. Mark, F. Wächtler, L. Santos, and F. Ferlaino, *Nature Physics* **14**, 442 (2018).
- [17] D. Petter, G. Natale, R. M. W. van Bijnen, A. Patscheider, M. J. Mark, L. Chomaz, and F. Ferlaino, *Phys. Rev. Lett.* **122**, 183401 (2019).
- [18] L. Tanzi, E. Lucioni, F. Famà, J. Catani, A. Fioretti, C. Gabbanini, R. N. Bisset, L. Santos, and G. Modugno, *Phys. Rev. Lett.* **122**, 130405 (2019).
- [19] F. Böttcher, J.-N. Schmidt, M. Wenzel, J. Hertkorn, M. Guo, T. Langen, and T. Pfau, *Phys. Rev. X* **9**, 011051 (2019).
- [20] L. Chomaz, D. Petter, P. Ilzhöfer, G. Natale, A. Trautmann, C. Politi, G. Durastante, R. M. W. van Bijnen, A. Patscheider, M. Sohmen, M. J. Mark, and F. Ferlaino, *Phys. Rev. X* **9**, 021012 (2019).
- [21] N. Meyer, H. Proud, M. Perea-Ortiz, C. O’Neale, M. Baumert, M. Holynski, J. Kronjäger, G. Barontini, and K. Bongs, *Phys. Rev. Lett.* **119**, 150403 (2017).
- [22] S. Serafini, M. Barbiero, M. Debortoli, S. Donadello, F. Larcher, F. Dalfovo, G. Lamporesi, and G. Ferrari, *Phys. Rev. Lett.* **115**, 170402 (2015).
- [23] L. Klaus, T. Bland, E. Poli, C. Politi, G. Lamporesi, E. Casotti, R. N. Bisset, M. J. Mark, and F. Ferlaino, *Nature Physics* **18**, 1453 (2022).
- [24] Here we use the normalisation and sign convention  $\mathcal{F}_{xy}(\cdot) = \int(\cdot)e^{-i(k_x x + k_y y)} dx dy$  for the direct Fourier Transform in two spatial dimensions, resulting in the inverse  $\mathcal{F}_{xy}^{-1}(\cdot) = 1/(2\pi) \int(\cdot)e^{i(k_x x + k_y y)} dk_x dk_y$ .
- [25] B. C. Mulkerin, D. H. J. O’Dell, A. M. Martin, and N. G. Parker, *Journal of Physics: Conference Series* **497**, 012025 (2014).
- [26] Note that in the dipolar gases literature  $\beta$  is often labelled as  $e_{dd}$ .
- [27] A. Villois and D. V. Skryabin, *Opt. Express* **27**, 7098 (2019).
- [28] M. Wenzel, F. Böttcher, J.-N. Schmidt, M. Eisenmann, T. Langen, T. Pfau, and I. Ferrier-Barbut, *Phys. Rev. Lett.* **121**, 030401 (2018).
- [29] S. B. Prasad, N. G. Parker, and A. W. Baggaley, *Phys. Rev. A* **109**, 063323 (2024).
- [30] B. C. Mulkerin, R. M. W. van Bijnen, D. H. J. O’Dell, A. M. Martin, and N. G. Parker, *Phys. Rev. Lett.* **111**, 170402 (2013).
- [31] F. Baronio, S. Wabnitz, and Y. Kodama, *Phys. Rev. Lett.* **116**, 173901 (2016).
- [32] W. J. Kwon, G. Del Pace, K. Khani, L. Galantucci, A. Muzi Falconi, M. Inguscio, F. Scazza, and G. Roati, *Nature* **600**, 64 (2021).